

Spectroscopy of three strongly coupled flux qubits

A. O. Niskanen,^{1,2,*} K. Harrabi,¹ F. Yoshihara,³ Y. Nakamura,^{1,3,4} and J. S. Tsai^{1,3,4}

¹CREST-JST, Kawaguchi, Saitama 332-0012, Japan

²VTT Technical Research Centre of Finland, Sensors, POB 1000, 02044 VTT, Finland

³The Institute of Physical and Chemical Research (RIKEN), Wako, Saitama 351-0198, Japan

⁴NEC Fundamental Research Laboratories, Tsukuba, Ibaraki 305-8501, Japan

(Received 19 September 2006; published 5 December 2006)

We have carried out spectroscopic measurements of a system of three strongly coupled four-junction flux qubits. The samples studied cover a wide range of parameters with the coupling energy between neighboring qubits varying between 0.75 GHz and 6.05 GHz. The observed complicated spectra agree well with eight-level theory. The experiments are relevant for the realization of a tunable coupling between qubits.

DOI: [10.1103/PhysRevB.74.220503](https://doi.org/10.1103/PhysRevB.74.220503)

PACS number(s): 74.50.+r, 03.67.Lx, 85.25.Cp

The potential realization of a full-scale quantum computer requires the ability of coupling multiple qubits together preferably so that the coupling can be turned on and off at will. In the context of Josephson junction qubits there are a number of promising theoretical suggestions¹⁻³ as well as already several experiments with coupled qubits.⁴⁻¹¹ In order for a quantum computer to be truly scalable it must be possible to couple many qubits together without degrading the coherence time severely. Tunable coupling has not been so far demonstrated in an experiment where the coherence time would be equally good as in the case of so-called optimally biased qubits.¹²⁻¹⁵ A problem common with many coupling methods is that in order to realize a two-qubit gate the biases need to be switched away from the region in the parameter space where the decoherence is minimal. In other words, while the coupling between two (or more) qubits is strengthened, the coupling between the qubits and the environment is, in many cases, also strengthened.

This Rapid Communication describes spectroscopic experiments on three strongly coupled flux qubits, which are relevant, for instance, for the scheme suggested in Ref. 16. In that scheme the parametric coupling of two detuned optimally biased flux qubits is realized through the microwave modulation of their tunable mutual inductance realized using a third qubit. Thus, the system we study is a set of three antiferromagnetically coupled flux qubits. When the flux threading the qubits is near the half-flux-quantum point (modulo flux quantum Φ_0) the system of three qubits is reasonably well described by the Hamiltonian

$$H = -\frac{1}{2} \sum_{j=1}^3 (\Delta_j \sigma_x^j + \epsilon_j \sigma_z^j) + \sum_{k=1}^3 \sum_{l=k+1}^3 J_{kl} \sigma_z^k \sigma_z^l, \quad (1)$$

where $\epsilon_j = 2I_{pj}(\Phi_j - \Phi_0/2)$ is the energy bias of qubit j controllable through the flux Φ_j threading the qubit loop. Near the half-flux-quantum point each qubit experiences a double-well potential and the tunneling energy through the potential barrier separating the wells is Δ_j . The wells correspond to currents of magnitude I_{pj} circulating in opposite directions along the loop, and the above Hamiltonian is actually written in this circulating current basis. The antiferromagnetic interaction between the qubits k and l is characterized by the coupling strength $J_{kl} = M_{kl} I_{pk} I_{pl}$ where M_{kl} is the mutual inductance.

A sample realizing such a system is shown in Fig. 1. The interesting part of the sample consists of three four-Josephson-junction flux qubits, similar to those studied individually in Refs. 13 and 15, coupled together by sharing one edge of the superconducting loop. Qubits 1 and 2 are thus expected to be weakly coupled due to small geometric inductance whereas each of them is expected to be strongly coupled to qubit 3 through kinetic inductance. Each qubit has one smaller Josephson junction whose area is about $\alpha \approx 0.5$ times smaller than that of the larger junctions having areas of about $200 \text{ nm} \times 400 \text{ nm}$. The qubits are coupled to a four-junction readout superconducting quantum interference device (SQUID) consisting of the three larger loops. The SQUID can be seen as a dc SQUID whose junctions are replaced by dc SQUIDs. This design was chosen in order to reduce the influence of the inevitable noise in the bias current. The coupling of the qubits to the SQUID is also through kinetic inductance. Since the different states of the qubits correspond to different magnetic field configurations in the SQUID loops, we expect a finite population of the excited states to result in a small but detectable change of the switching current of the SQUID.

The samples used in this study were fabricated out of Al using standard shadow evaporation through a Ge-enforced mask patterned with e -beam lithography. The designs of samples *A*, *B*, and *C* were slightly different. In sample *A* we used an on-chip capacitor to shunt the SQUID.^{13,15,18} In samples *B* and *C* this capacitor was removed in order to clean up the measurable spectrum from resonances such as LC resonances and the plasma resonance. An additional benefit of removing the large superconducting shunt capacitor was improved flux stability. Both designs had no on-chip bias resistors but instead we used an on-chip LC filter consisting of a long superconducting line¹⁷ and a superconducting capacitor. The two plates of the Al parallel-plate capacitor were defined in a separate e -beam lithography step and the insulator was formed by heavily oxidizing the bottom layer. The estimated cutoff of the filter was 100–200 MHz. In sample *A* the inductor was about 15 mm long and 600 nm wide, resulting in a transmission line resonance around 10 GHz. The shorter line of samples *B* and *C* (3.2 mm) gives a resonance around 20 GHz. The oxidation of the junction was done using a mixture of O_2 (10%) and Ar (90%) between depositions of the 20-nm and 30-nm Al layers. For the

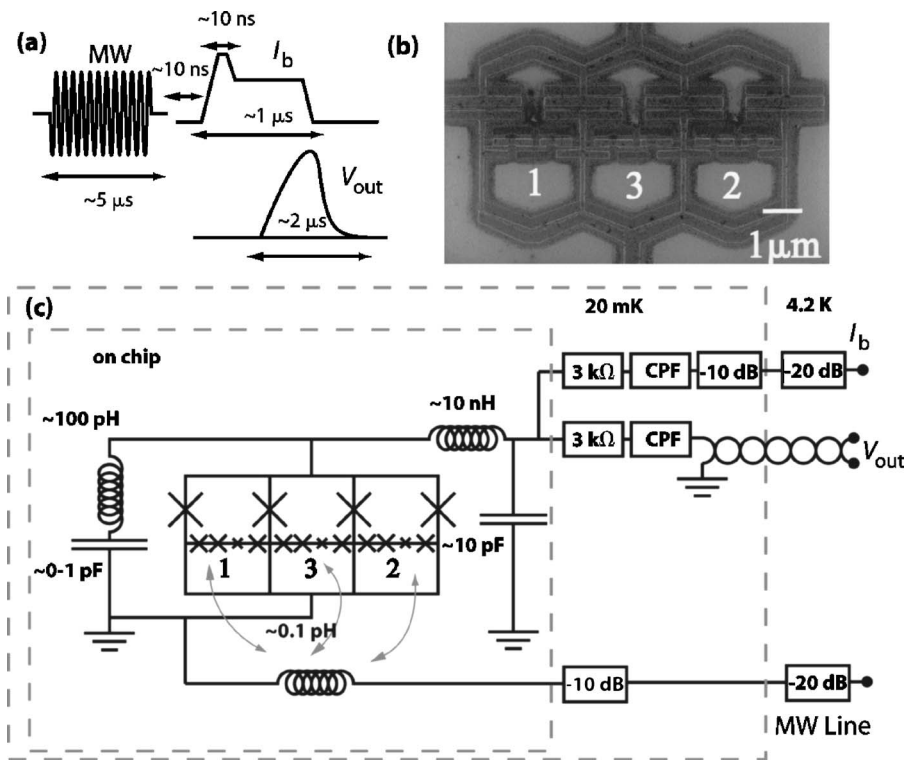


FIG. 1. (a) Timing diagram and the principle of the measurement. (b) Scanning electron microscope (SEM) image of the sample. (c) Detailed wiring. CPF stands for copper powder filter.

microwave line and bonding pads we used evaporated gold film defined by optical lithography. Part of the microwave line also had an Al layer. The measurements were carried out in a dilution refrigerator with a base temperature around 20 mK. The fridge had a triple μ -metal magnetic shield.

The principle of the measurement¹⁸ is shown in Fig. 1. First a microwave pulse of typically $5 \mu\text{s}$ duration is applied to the microwave line on chip. Then immediately after this a current pulse of about 5–10 ns is applied to the SQUID. The height is chosen so that the SQUID switches about every second time. The current pulse is followed by a trailing plateau whose height is about 70% of the switching current. The purpose of the plateau is to maintain the SQUID in the voltage state if and only if the SQUID switched. By repeating each measurement typically 10^4 times and counting the relatively slow voltage pulses (few μs) we can deduce the switching probability P_{sw} under particular circumstances. To supply the flux bias to the qubits we used an external coil capable of inducing about 20 G. To carry out spectroscopy on the qubits we first located them in the flux space. The basic measurement was then carried out by sweeping the microwave frequency and magnetic field and repeating the above-mentioned measurement scheme. At each flux point the height of the current pulse was adjusted to get roughly the same P_{sw} in the absence of the microwave. The qubits (as well as other resonances) cause deviations from this probability, enabling the characterization of the spectrum of the three-qubit system. The application of current through the SQUID changes the magnetic fluxes experienced by the qubits, and this shift is assumed to be adiabatic. The deviation may be either up or down depending on the configuration of

the circulating currents after the adiabatic shift.

Figure 2 is an example of such a spectroscopic measurement on sample A. The horizontal lines are resonances due to the presence of on-chip capacitors. The strong resonance around 10 GHz is most likely a half-wavelength resonance in the long bias line. However, the qubits are clearly visible and form a rich spectrum. The top panel shows the measured spectrum only while in the bottom panel a theoretical calculation of the spectrum is shown on top of the measured spectrum. The calculation is simply done numerically using Eq. (1) by finding the excited-state eigenvalues and subtracting the ground-state eigenvalue from them. It is worthwhile stressing that the theoretical part is not based on a fitting procedure such that there may be a considerable amount of error in all the parameters, but the agreement does seem at least qualitatively very good. The persistent currents denoted by \tilde{I}_{pk} in the figure captions are the nominal values used in the computation and do not account for the shielding effect due to the readout SQUID. The actual persistent currents I_{pk} are expected to be significantly larger and thus the mutual inductances M_{jk} are expected to be smaller than what it seems considering the currents \tilde{I}_{pk} since M_{jk} is inversely proportional to I_{pk} for a given coupling J_{jk} . Based on the rather high measured normal-state resistivity of $\rho_{4.2\text{ K}}^{\text{Al}} = 11 \mu\Omega \text{ cm}$ we estimate using¹⁹ $L_{\text{kin}} = (\Phi_0 e R_n) / (\pi^2 \Delta_{\text{BCS}})$ that $M_{13} = M_{23} = 31 \text{ pH}$. For instance in Ref. 19 the resistivity seems to be about 7 times smaller while, e.g., in Ref. 20 it is about half of our value. In order for this to be consistent with the coupling energy the shielding should be about 11%. Due to the coupling, we observe more than three levels and everywhere the spectrum lines cannot be simply associated with a particular

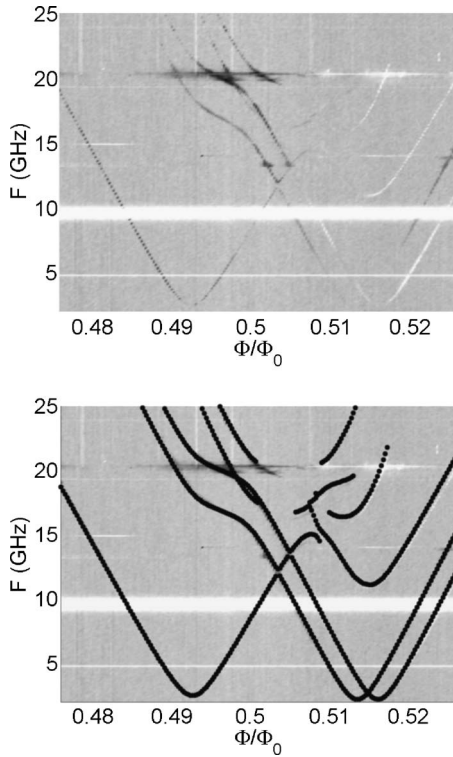


FIG. 2. Spectroscopy of sample A. The top panel is an intensity plot of P_{sw} while the bottom panel includes the numerically calculated spectrum. Black dots denote excitation energies from the ground state $|0\rangle$ for the states $|\Psi\rangle$ with $|\langle 0|\sum_{j=1}^3\sigma_z^j|\Psi\rangle|^2 \geq 0.002$. In the calculation we used $\Delta_1/h=2.2$ GHz, $\Delta_2/h=2.2$ GHz, $\Delta_3/h=2.5$ GHz, $J_{13}/h=J_{23}/h=2.05$ GHz, $J_{12}=0$ GHz, $\Delta\Phi_1/\Phi_0=-0.0128$, $\Delta\Phi_2/\Phi_0=-0.0102$, $\tilde{I}_{p1}=194$ nA, $\tilde{I}_{p2}=194$ nA, and $\tilde{I}_{p3}=179$ nA. The lines shared by the qubits have dimensions of $1.35 \mu\text{m} \times 30 \text{nm} \times 160 \text{nm}$. Qubits 1 and 2 have $\alpha=0.5$ while qubit 3 has $\alpha=0.475$. Oxidation was done with 25 mTorr for 5 min. Switching measurement yields $I_{c,\text{max}}^{\text{SQUID}} \approx 8.8 \mu\text{A}$. The maximum contrast is about 15%.

qubit. Roughly speaking, the line having a minimum of about 2.5 GHz corresponds to qubit 3 and the other two minima around 2.2 GHz correspond to qubits 1 and 2. This can be justified by noting that qubit 3 is the only one coupled strongly to two other qubits; see, e.g., the bending of the second and third levels around $\Phi/\Phi_0=0.49$ where the current in qubit 3 changes direction. The slightly higher tunneling energy is because qubit 3 was fabricated with $\alpha=0.475$ as the designed ratio of the large and small junction area, while qubits 1 and 2 had $\alpha=0.5$. Since we are using only one control magnet, we can write the flux biases as $\Phi_j=\Phi+\Delta\Phi_j$. The small offsets $\Delta\Phi_j$ are, in the absence of trapped vortices, due to slight differences in the areas. Since we only work in rather small range around $\Phi_0/2$, the effect of area difference on the slope is not significant. We choose a convention where $\Delta\Phi_3=0$. Note, however, that due to the interaction between qubits, not even qubit 3 has a minimum exactly at $\Phi_0/2$. The lack of visibility of some levels at certain fields can be understood as a small transition matrix element. In fact, in the theoretical calculation we have plotted only levels $|\Psi\rangle$ for which $|\langle 0|\sum_{j=1}^3\sigma_z^j|\Psi\rangle|^2 \geq 0.002$.

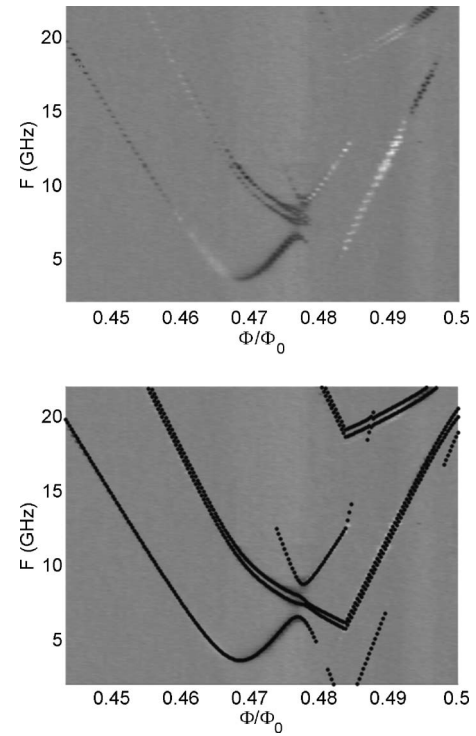


FIG. 3. Spectroscopy of sample B. The parameters used in the calculation are $\Delta_1/h=1.3$ GHz, $\Delta_2/h=1.0$ GHz, $\Delta_3/h=3.6$ GHz, $J_{13}/h=J_{23}/h=6.05$ GHz, $J_{12}=0$ GHz, $\Delta\Phi_1/\Phi_0=-0.0096$, $\Delta\Phi_2/\Phi_0=-0.010$, $\tilde{I}_{p1}=156$ nA, $\tilde{I}_{p2}=156$ nA, and $\tilde{I}_{p3}=124$ nA. We only show levels for which $|\langle 0|\sum_{j=1}^3\sigma_z^j|\Psi\rangle|^2 \geq 0.0001$. The lines shared by the qubits have dimensions of $1.35 \mu\text{m} \times 20 \text{nm} \times 100 \text{nm}$. Qubits 1 and 2 have $\alpha=0.5$ while qubit 3 has $\alpha=0.45$. Oxidation was done with 25 mTorr for 10 min. We get $I_{c,\text{max}}^{\text{SQUID}} \approx 20.2 \mu\text{A}$. The maximum contrast is about 15%.

Figures 3 and 4 illustrate measured spectra for samples B and C. As can be seen, the calculations again agree extremely well with the measurement. Together with sample A the samples cover a very wide range of parameters. Note that the sizes of the anticrossings depend not only on the coupling energy but also on the distance from the optimal point. It is especially noteworthy that the coupling energy can be made as large as 6 GHz without using coupling junctions.⁹ The shielding effect and the coupling inductance are expected to be very large in these samples since the line shared by the qubits and SQUID is made thinner and narrower than in sample A. A prediction based on normal-state resistance yields the estimate $M_{13}=M_{23}=74$ pH. In order to explain the observed coupling energy the shielding in sample B should be about 40% and in sample C about 14%. These numbers are reasonable although hard to verify. The scaling of these percentages is correct as a function of $I_{c,\text{max}}^{\text{SQUID}}$; i.e., a large critical current of the SQUID means also a large shielding current due to the SQUID.

Even though the predicted kinetic inductances are large, one may suspect that the large coupling could be partially due to a shared Josephson inductance L_J . Namely, a fraction of the persistent current of each qubit could flow through the large junctions of the SQUID. However, this effect may only reduce the coupling from the prediction based on shared ki-

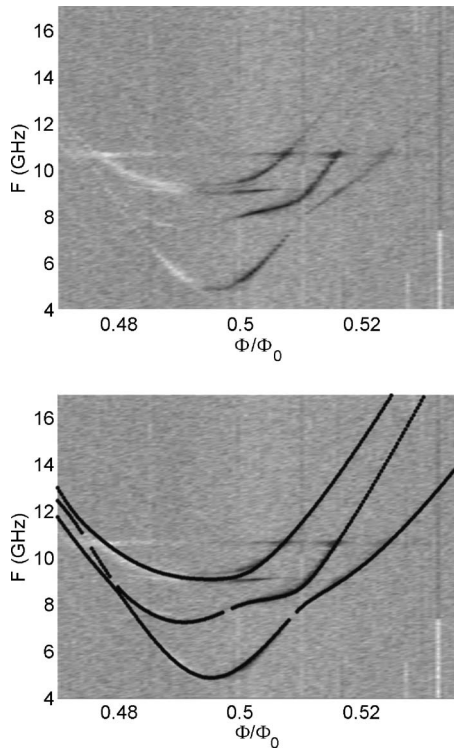


FIG. 4. Spectroscopy of sample *C*. In the calculation we used $\Delta_1/h=5.0$ GHz, $\Delta_2/h=7.5$ GHz, $\Delta_3/h=8.2$ GHz, $J_{13}/h=0.79$ GHz, $J_{23}/h=0.755$ GHz, $J_{12}=0$ GHz, $\Delta\Phi_1/\Phi_0=-0.0041$, $\Delta\Phi_2/\Phi_0=-0.0087$, $\tilde{I}_{p1}=81$ nA, $\tilde{I}_{p2}=78$ nA, and $\tilde{I}_{p3}=64$ nA. Levels with $|\langle 0|\sum_{j=1}^3\sigma_z^j|\Psi\rangle|^2 \geq 0.005$ are shown. The different slopes are due to the fact that qubits 1 and 2 were designed with $\alpha=0.5$ and $\alpha=0.475$ while qubit 3 has $\alpha=0.45$. The lines shared by the qubits have dimensions of $1.35 \mu\text{m} \times 20 \text{ nm} \times 100 \text{ nm}$. Oxidation was done with 35 mTorr for 10 min. We get $I_{c,\text{max}}^{\text{SQUID}} \approx 5.4 \mu\text{A}$. The maximum contrast is about 5%.

netic inductance since the effect of the large shared L_J is canceled by the fact that the fraction of the persistent currents flowing through the large junctions decreases with increasing L_J . Explicitly, if the currents of two qubits k and l can flow through two inductances $2L_1$ (kinetic) and $2L_2$ (kinetic plus Josephson), and if half of these inductances are shared with the other qubit, then $J_{kl}=L_1L_2/(L_1+L_2)I_{pk}I_{pl}$. This clearly is maximal for $L_2 \rightarrow \infty$. An additional experimental point related to this is that in all samples we reproduced the measured spectrum well by setting the direct coupling of qubits 1 and 2 to zero even though their currents have a chance to flow through a “shared” large Josephson junction.

In conclusion we have carried out spectroscopic measurements of three strongly coupled flux qubits. We demonstrated that one can achieve a wide range of coupling strengths using kinetic inductance for the coupling. The relatively high coupling energy is attributable to the rather large normal-state resistivity of our aluminum film. We find that the effective three-qubit Hamiltonian describes the measured spectrum well. Based on our experience it is possible to reproducibly fabricate qubits whose flux biases differ by less than 1% even when using only a single bias coil. The different effective area of qubit 3 in all samples is due to the fact that its position is not symmetric with respect to other qubits. However, it is possible to tune the area very accurately by adjusting the layout. Similar areas enable optimal point biasing of many qubits without strongly coupled independent bias lines. The experiments reported in this paper are a step towards the tunable coupling of flux qubits. The parameters of sample *C* in particular are very close to those required for the parametric coupling using a third qubit.¹⁶

We would like to thank M. Grajcar for useful discussions.

*Electronic address: niskanen@frl.cl.nec.co.jp

- ¹C. Rigetti, A. Blais, and M. Devoret, Phys. Rev. Lett. **94**, 240502 (2005).
- ²P. Bertet, C. J. P. M. Harmans, and J. E. Mooij, Phys. Rev. B **73**, 064512 (2006).
- ³M. Grajcar, Y.-X. Liu, F. Nori, and A. M. Zagoskin, Phys. Rev. B **74**, 172505 (2006).
- ⁴Yu. A. Pashkin *et al.*, Nature (London) **421**, 823 (2003).
- ⁵T. Yamamoto, Yu. A. Pashkin, O. Astafiev, Y. Nakamura, and J. S. Tsai, Nature (London) **425**, 941 (2003).
- ⁶A. J. Berkley *et al.*, Science **300**, 1548 (2003).
- ⁷J. B. Majer, F. G. Paauw, A. C. J. ter Haar, C. J. P. M. Harmans, and J. E. Mooij, Phys. Rev. Lett. **94**, 090501 (2005).
- ⁸R. McDermott *et al.*, Science **307**, 1299 (2005).
- ⁹M. Grajcar *et al.*, Phys. Rev. Lett. **96**, 047006 (2006).
- ¹⁰S. H. W. van der Ploeg *et al.*, cond-mat/0605588 (unpublished).

- ¹¹M. Steffen *et al.*, Science **313**, 1423 (2006).
- ¹²D. Vion *et al.*, Science **296**, 886 (2002).
- ¹³P. Bertet *et al.*, Phys. Rev. Lett. **95**, 257002 (2005).
- ¹⁴A. Wallraff *et al.*, Phys. Rev. Lett. **95**, 060501 (2005).
- ¹⁵F. Yoshihara, K. Harrabi, A. O. Niskanen, Y. Nakamura, and J. S. Tsai, Phys. Rev. Lett. **97**, 167001 (2006).
- ¹⁶A. O. Niskanen, Y. Nakamura, and J. S. Tsai, Phys. Rev. B **73**, 094506 (2006).
- ¹⁷J. Claudon, F. Balestro, F. W. J. Hekking, and O. Buisson, Phys. Rev. Lett. **93**, 187003 (2004).
- ¹⁸I. Chiorescu, Y. Nakamura, C. J. P. M. Harmans, and J. E. Mooij, Science **299**, 1869 (2003).
- ¹⁹A. C. J. ter Haar, Ph.D. Thesis, Delft University of Technology, 2005.
- ²⁰F. Balestro, J. Claudon, J. P. Pekola, and O. Buisson, Phys. Rev. Lett. **91**, 158301 (2003).